COMPUTATIONAL MECHANICS
WCCM VI in conjunction with APCOM'04, *Sept. 5-10, 2004, Beijing, China*

Numerical Analyses of Transonic Fluid/Structure Interaction in Aircraft Engineering

Guowei Yang [1]*, Shigeru Obayashi [2]

[1] *Institue of Mechanics, Chinese Academy of Sciences, Beijing, 100080, China*
[2] *Institute of Fluid Science, Tohoku University, Sendai, 980-8577, Japan*
e-mail: gwyang@imech.ac.cn., obayashi@ieee.org

Abstract Through the coupling between aerodynamic and structural governing equations, a fully implicit multiblock aeroelastic solver was developed for transonic fluid/structure interaction. The Navier-Stokes fluid equations are solved based on LU-SGS (lower-upper symmetric Gauss-Seidel) time-marching subiteration scheme and HLLEW (Harten-Lax-van Leer-Einfeldt-Wada) spatial discretisation scheme and the same subiteration formulation is applied directly to the structural equations of motion in generalized coordinates. Transfinite interpolation (TFI) is used for the grid deformation of blocks neighboring the flexible surfaces. The infinite plate spline (IPS) and the principal of virtual work are utilized for the data transformation between fluid and structure. The developed code was first validated through the comparison of experimental and computational results for the AGARD 445.6 standard aeroelastic wing. Then the flutter character of a complete aircraft configuration was analyzed.

Key words: fluid/structure interaction, flutter, numerical simulation

INTRODUCTION

In the last decade, numerical analyses of nonlinear transonic fluid/structure interaction such as flutter have been extensively studied by solving Euler/Navier-Stokes equations coupled with the structural equations of motion [1-4]. However, in these methods, the flow governing equations are only loosely coupled with structural equations of motion, namely, after the aerodynamic loads are determined by solving the flow governing equations, the structural model is used to update the position of body. The coupling contains the error of one time step, thus these methods are always only first-order accuracy in time regardless of the temporal accuracy of the individual solvers of the flow and structural equations.

Tightly coupled aeroelastic approach was first put forward by Alonso and Jameson [5] for 2-D Euler aeroelastic simulation, called dual-time implicit-explicit method. In each real time step, the time-accurate solution is solved by explicit Runge-Kutta time-marching method for a steady problem, so all of convergence acceleration techniques such as multigrid, residual averaging and local time-step can be implemented in the calculation. In general, about 100 pseudo-time steps are needed for the explicit iterations to ensure adequate convergence, thus the method is still very time-consuming, so far as the authors know only 3-D Euler results were reported recently [6]. Based on the same thought, G. S. L. Goura et al. [7] constructed a first-order implicit time-marching scheme as well as only first-order spatial discretisation in implicit side for the solution of a pseudo steady flow. The second-order temporal and spatial accuracy can be maintained as pseudo steady flow convergence. Euler equations were chosen as the aerodynamic governing equations due to the limitation of computational time.

Melville et al [8] proposed a fully implicit aeroelastic solver between the fluids and structures, in which a second-order approximately factorization scheme with subiterations was performed for the flow governing equations, and the structural equations were cast in an iterative form. Because the restricted number of iterations cannot remove sequencing effects and factorization errors completely at every time

step and a relatively small time step was used in their calculation. Nevertheless, a fully implicit aeroelastic Navier-Stokes solver with three subiterations has succeeded in the flutter simulation for an aeroelastic wing [9].,

In the flutter calculation, due to the deformation of aeroelastic configuration, adaptive dynamic grid needs to be generated at each time step. At present, most of aeroelastic calculations are only done for an isolated wing with single-block grid topology. For the simple flexible geometry, the grid can be completely regenerated with an algebraic method [1] or a simple grid deformation approach [9]. For the complicated aerodynamic configurations, multiblock grids are usually generated for steady flow simulation. However, for aeroelastic application it is impossible to regenerate multiblock grids at each time step due to the limitation of computational cost. Multiblock grid deformation approachs need to be used. Recently Potsdam and Guruswamy [10] put forward a multiblock moving grid approach, which uses a blending method of a surface spline approximation and nearest surface point movement for block boundaries, and transfinite interpolation (TFI) for the volume grid deformation. Wong et al. [11] also established a multiblock moving mesh algorithm. The spring network approach is utilized only to determine the motion of the corner points of the blocks and the TFI method is applied to the edge, surface and volume grid deformations

In addition, structural data may be provided with plate model, but the flow calculations are carried out for the full geometry. The interpolation between fluid and structure grids is required. Infinite and finite surface splines [12, 13] developed for the plate aerodynamics and plate structural model are still main interpolation tools, only the aerodynamic grid needs to be projected on the surface of structural grid before interpolation. Goura et al [14] recently suggested an interpolation method of constant volume transformation (CVT) for the data exchange between fluids and structures based on the local grid information

In the present paper, a fully implicit multiblock Navier-Stokes aeroelastic solver was developed based on the single-block aeroelastic code implemented by the authors [15, 16]. The purpose of the present work is to simulate the fluid/structure interaction for complex configuration. First the flutter boundaries and frequencies for the AGARD 445.6 standard aeroelastic wing were predicted and compared with experimental data to validate the developed aeroelastic code. Then the flutter character for a complicated aircraft was analyzed.

GOVERNING EQUATIONS

1.Aerodynamic Governing Equations In the paper, freestream density, freestream velocity and the root chord or mean aerodynamic chord length are chosen as character quantities. Aerodynamic governing equations are the unsteady, three-dimensional thin-layer Navier-Stokes equations in strong conservation law form, which can be written in curvilinear space ξ, η, ζ and τ in non-dimensional form as

$$\partial_\tau \hat{Q} + \partial_\xi F + \partial_\eta G + \partial_\zeta H = \mathrm{Re}^{-1} \partial_\zeta H_v + S_{GCL} \tag{1}$$

In the formulation, the viscosity coefficient μ in H_v is computed as the sum of laminar and turbulent viscosity coefficients, which are evaluated by the Sutherland's law and Baldwin-Lomax model with the Degani-Schiff modification. For multiblock grid calculation, the turbulence model is difficult to be applied to the blocks having no solid surface, because the model needs not only the local flowfield but also its corresponding gradient values on the wall surface. In addition, the thin layer approximation may be unsuitable for general multiblock grids in which one block may have more than two solid surfaces. Therefore, the multiblock grids are carefully generated so as to have a single solid surface

The source term S_{GCL} in Equation 1 is obtained from the geometric conservation law [17] for moving mesh, which is defined as

$$S_{GCL} = Q\left[\partial_t J^{-1} + (\xi_t / J)_\xi + (\eta_t / J)_\eta + (\zeta_t / J)_\zeta\right] \tag{2}$$

STRUCTURAL DYNAMIC GOVERNING EQUATIONS

Second-order linear structural dynamic governing equations after normalized similar to the flow governing equation can be written as

$$[M]\{\ddot{d}\}+[K]\{d\}=\{F\} \tag{3}$$

where $[M]$, $[K]$ are the non-dimensional mass and stiffness matrices, respectively. $\{F\}$, $\{d\}$ are the aerodynamic load and displacement vectors, respectively. In order to solve Equation 3, the Rayleigh-Ritz method is used. For specific aerodynamic configuration, the natural mode shapes and frequencies can be calculated by the finite-element analysis or obtained from experimental influence coefficient measurements. In this study, the data of natural mode shapes and frequencies are calculated by finite-element analysis. In general, only the first N modes are considered. With these first N modes we have an approximate decription of the displacement vector of the system given by

$$\{d\}=[\Phi]\{q\} \tag{4}$$

Since the natural modes are orthogonal with respect to both the mass and stiffness matrices, premultiplying Equation 3 by $[\Phi]^T$ yields structural equations in generalized coordinates

$$\ddot{q}_i+2\zeta_i\omega_i\dot{q}_i+\omega_i^2 q_i=[\Phi]_i^T F/M_i \tag{5}$$

where

$\omega_i^2=[\Phi]_i^T\{K\}[\Phi]$, $M_i=[\Phi]_i^T\{M\}[\Phi]$

The modal damping is readily added on the left hand side of Equation 5, where ζ_i is the damping ratio in the i th mode. The equation can be written as a first-order system by defining $S=[q,\dot{q}]$

$$\dot{S}+\begin{bmatrix}0 & -1\\ \omega_i^2 & 2\omega_i\varsigma_i\end{bmatrix}S=\begin{bmatrix}0\\ [\Phi]_i^T F/M_i\end{bmatrix} \tag{6}$$

NUMERICAL METHOD

LU-SGS method of Yoon and Jameson [18], employing a Newton-like subiteration, is used for solving Equation 1. Second-order temporal accuracy is obtained by utilizing three-point backward difference in the subiteration procedure. The numerical algorithm can be deduced as

$$\begin{aligned}&LD^{-1}U\Delta Q\\ &=-\phi^i\{(1+\phi)Q^p-(1+2\phi)Q^n+\phi Q^{n-1}\\ &-J\Delta\tau Q^p\left[(\xi_t/J)_\xi+(\eta_t/J)_\eta+(\zeta_t/J)_\zeta\right]^p\\ &+J\Delta\tau(\delta_\xi F^p+\delta_\eta G^p+\delta_\zeta(H^p-H_v^p))\}\end{aligned} \tag{7}$$

where

$L=\overline{\rho}I+\phi^i J\Delta\tau(A^+_{i-1,j,k}+B^+_{i,j-1,k}+C^+_{i,j,k-1})$, $D=\overline{\rho}I$

$U=\overline{\rho}I-\phi^i J\Delta\tau(A^-_{i+1,j,k}+B^-_{i,j+1,k}+C^-_{i,j,k+1})$

and

$\overline{\rho}=1+\phi^i J\Delta\tau(\overline{\rho}(A)+\overline{\rho}(B)+\overline{\rho}(C))$, $\phi^i=1/(1+\phi)$, $\Delta Q=Q^{p+1}-Q^p$

Here, $\phi=0.5$, and p denotes the subiteration number. The deduced subiteration scheme reverts to the standard LU-SGS scheme for $\phi=0$ and $p=1$. In fact, regardless of the temporal accuracy of the left hand of Equation 7, second-order time accuracy is maintained when the subiteration number tends to infinity

The inviscid terms in Equation 7 are approximated by modified third-order upwind HLLEW scheme of Obayashi et al [19]. For the isentropic flow, the scheme results in the standard upwind-biased flux-difference splitting scheme of Roe, and as the jump in entropy becomes large in the flow, the scheme turns into the standard HLLEW scheme. Thin-layer viscous term in Equation 7 is discretized by second-order central difference

In the multiblock-grid method, the Navier-Stokes equations are solved in each block separately. The calculations of convective and viscous fluxes at block boundaries need flowfield values of two grid points in abutting blocks, so the lagged flowfield always exists due to the lagged block boundary condition. Using the LU-SGS method, in the forward sweep, the correction of conserved variables ΔQ in the first-level halo cell is usually neglected. In the backward sweep, the correction of temporary variables $\Delta Q'$ obtained from the forward sweep can only be set to zero at block boundaries, which can produce larger error than the same code using a single-block grid. Rizzetta eta al [20] considered that the subiteration can eliminate errors from linearization, factorization, lagged boundary conditions, and lagged turbulence models.

The structural equations of motion in generalized coordinates of Equation 7 is discretized by a second order scheme with subiterations of reference [9] as

$$\begin{bmatrix} 1 & -\phi^i \Delta\tau \\ \phi^i \Delta\tau \omega_i^2 & 1+2\phi^i \omega_i \zeta_i \Delta\tau \end{bmatrix} \Delta S$$
$$= -\phi^i \{(1+\phi)S^p - (1+2\phi)S^n + \phi S^{n-1} \qquad (8)$$
$$+ \Delta\tau \begin{bmatrix} 0 & -1 \\ \omega_i^2 & 2\omega_i \zeta_i \end{bmatrix} S^p - \Delta\tau \begin{bmatrix} 0 \\ [\Phi]_i^T F^p / M_i \end{bmatrix} \}$$

where $\Delta S = S^{p+1} - S^p$

As $p \to \infty$, a full implicit second-order temporal accuracy scheme for aeroelastic computation is formed by the coupling solutions of Equation 7 and 8. For accurate multiblock-grid aeroelastic calculation, the subiteration method is very important not only for eliminating the lagged flowfield induced by lagged multiblock boundary condition but also for removing the sequencing effects between fluids and structures. However, in practical application, only finite subiterations can be used. For example, an approximately factored implicit solver with three subiterations was used in Ref. 9. Similarly, three subiterations are used for the present calculation. Since the restricted number of iterations does not remove sequencing effects and factorization errors at every time step completely, a proper time-step size needs to be evaluated by numerical tests

MULTIBLOCK GRID GENERATION AND DEFORMATION

1. Multiblock Grid Generation For complex aerodynamic configuration, the multiblock grid-generation challenges continuously for the community of computational fluid dynamics. Grid topology may be further limited due to the assumption of thin-layer approximation and the use of turbulence model. In the paper, one of the aircraft configurations calculated is shown in Fig. 1. The surface grid is first distributed, which contains 5 zones, 3 zones for fuselage and 2 zones for the main wing and the horizontal wing,respectively. Total 10 zones are distributed on the whole surface. An H-type multiblock grid with 40 blocks depicted in Fig. 2 can be chosen to satisfy the requirements. In the multiblock grid, the edge grids of each block are generated with a polynomial function, which is determined by the coordinates and direction derivatives of two endpoints of the edge grid line. The surface and volume grids of each blocks are generated sequentially with the two- and three dimensional TFI methods. Finally, two- and three-dimensional elliptic methods are applied to smooth surface and volume grid distributions, to adjust the orthogonality at boundaries and to keep the grid continuity between abutting blocks. For the H-type multiblock grid, an acceptable grid can be gotten even no use of the elliptic smoothing method.

2. Multiblock Grid Deformation For the above H-type multiblock grid topology with 40 blocks, only the blocks containing the aircraft surface and the blocks abutting the flexible aircraft need to be deformed. Other blocks can be fixed.

The TFI method [11] is applied to deform the grid blocks. Based on the known deformations of the flexible aircraft surface and the parameterized arc-length values of the original grid, 1-D, 2-D and 3-D TFI methods can be used to interpolate deformation values in inner grid points. Then the deformations are added to the original grid to obtain the new multiblock grid. For the small and moderate aeroelastic

deformation, the present method maintains the grid quality of the original grid and maximizes the re-usability of the original grid. For the full movement of horizontal wing, a simple sheared mesh is used and a gap is introduced between the fuselage and wing to allow sufficient space for the moving sheared mesh. The present solver assumes the oscillation of horizontal wing with small amplitude.

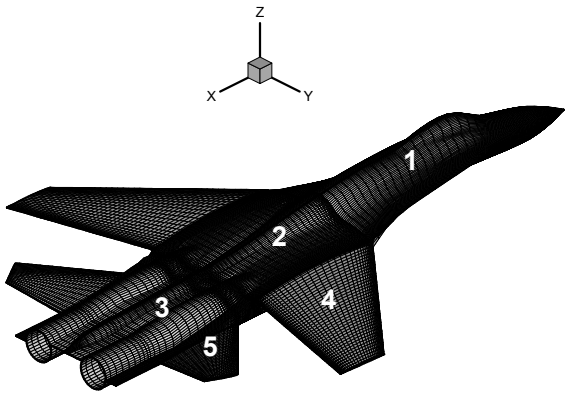

Fig. 1 Surface grid

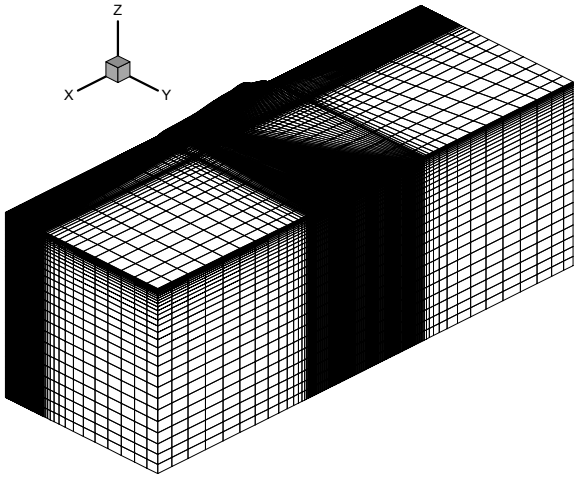

Fig. 2 Multiblock grid with 40 blocks

DATA TRANSFORMATION

In the present aeroelastic calculations, the structural modal data are provided with the plate model and only normal deformation is considered. However, the real geometry is used for the fluid solution. Then the problem of passing information between the fluid and structural grids becomes very complicated. In the paper, the fluid grid is first projected to the surface of structural grid. The deformations on the projected fluid grid points are interpolated by the infinite plate spline (IPS) [12].

IPS is to obtain an analytic function $w(x, y)$, which passes through the given structural deflections of N points $w_i = w(x_i, y_i)$. The static equilibrium equation of $D\nabla^4 w = q$ should be satisfied, where D is the plate elastic coefficient, q is the distributed load on the plate. The solution by superposition of fundamental functions can be written as

$$w(x, y) = a_0 + a_1 x + a_2 y + \sum_{i=1}^{N} F_i r_i^2 \ln r_i^2 \tag{9}$$

where $r_i^2 = (x - x_i)^2 + (y - y_i)^2$

The $N + 3$ coefficients of $(a_0, a_1, a_3, F_1, F_2, \cdots, F_N)$ in Equations 9 can be solved through the function passes the given structural deflections of N and three additional conditions of the conservation of total force and moment

$$\sum_{i=1}^{N} F_i = 0\,,\ \sum_{i=1}^{N} x_i F_i = 0 \ \text{ and } \ \sum_{i=1}^{N} y_i F_i = 0 \tag{10}$$

Then the deformations of aerodynamic grid points can be evaluated with the function (9). The above linear displacement transformation can be written in the form $\delta S_a = [G]\delta S_s$, where δS_a and δS_s are the displacement vectors defined on the aerodynamic grid and the structural grid, respectively

The force transformation from the fluid to structural grids can be calculated with the principle of virtual work of $F_s = [G]^T F_a$, where F_s and F_a represent the forces on the structural and fluid grids, respectively. The principle of virtual work can guarantee the conservation of energy between the fluid and structural systems.

In the practical application, the LU decompositions of the coefficients matrix and its transpose matrix of the equation groups of (9) and (10), $a_0, a_1, a_3, F_1, \ldots, F_N$ as unknown quantities, are pre-calculated and stored in the code. In general, interpolations are applied on the fuselage and wing separately since the deformation on the wing and the body may have different character.

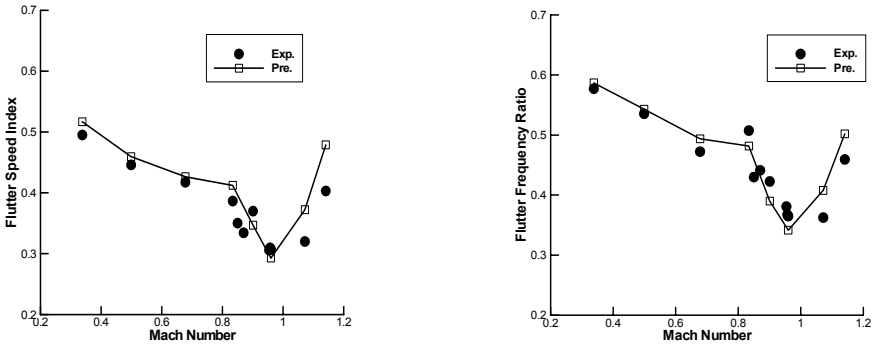

Fig. 3 Flutter speed and frequency for the AGARD standard aeroelastic wing

RESULTS AND DISCUSSIONS

1. AGRAD 445.6 Wing Aeroelastic wind-tunnel experiment is intrinsically destructive and hence much more expensive than a similar rigid-body experiment. Therefore, it is hard to find a suitable experimental data to validate the developed aeroelastic solver. The unique complete aeroelastic experiment is available for the AGARD 445.6 standard aeroelastic wing [21], which has been used to validate flutter simulations in most of publications. The disadvantage of the test is that the nonlinear character is relatively weak due to a thin wing, and thus linear, Euler and Navier-Stokes equations all can predict good results comparing with experimental data. However, in the absence of a better experiment, the experiment is still used to evaluate the current method

The AGARD 445.6 wing model was constructed of laminated mahogany and was essentially homogeneous. The wing has an aspect ratio 1.6525, a taper ratio of 0.6576, a quarter-chord swept angle of 45 deg and a NACA 65A004 airfoil section.

The first four structural modes and natural frequencies provided in the reference [21] are used for the present computations and a nondimensional time step is taken as $\Delta t = 0.05$. All simulations are started from its corresponding steady flow. Each Mach number is run for several dynamic pressures to determine the flutter point. As the dynamic pressure is varied, the freestream density and Mach number are held fixed and Reynolds number is allowed to vary. At $t = 0$, a small initial velocity pertubation of 0.0001 for the first bending mode is applied to the wing

The flutter boundary and frequency over the Mach number range of 0.338 to 1.141 are calculated and compared with experimental data in Fig. 3. The typical transonic dip phenomenon is well captured. In the subsonic and transonic range, the calculated flutter speeds and frequencies agree well with experimental data, however, in the supersonic range, the present calculation overpredicts the experimental flutter points similar to other computations. To investigate the possible sources for the difference between the experiment and computation, Melville et al [9] examined the effects of various computational parameters, using 14 modes in structural model, using different numerical schemes and changing the location of the computational transition location downstream from the leading edge to the 30% chord location. But only minimal effects of these changes were observed in the flutter response, it is not significant enough to explain the discrepancies between the computations and experiment. So their conclusion is that the actual physical conditions in the experiment may not be properly reflected in the computations. Significant changes in flutter speed and frequency could originate in a small difference in Mach numbers in the supersonic flow region. Therefore, any small experimental error in Mach number could lead to significant differences between computed and experimental flutter properties.

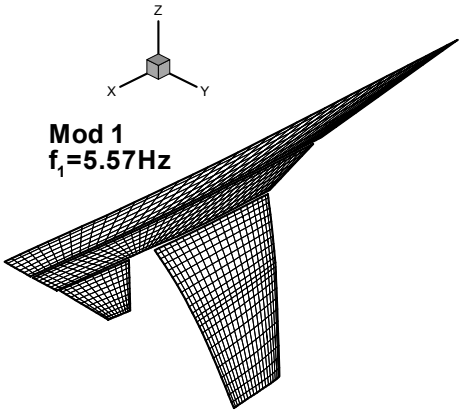

(4a)

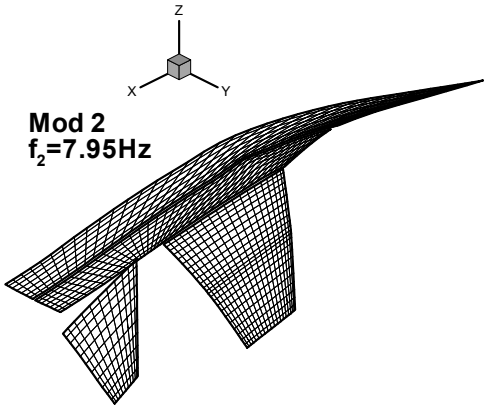

(4b)

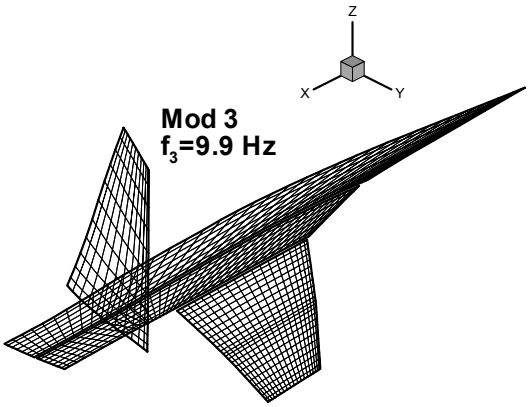

(4c)

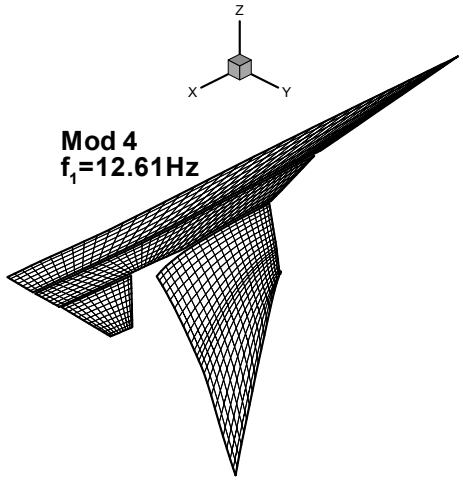

(4d)

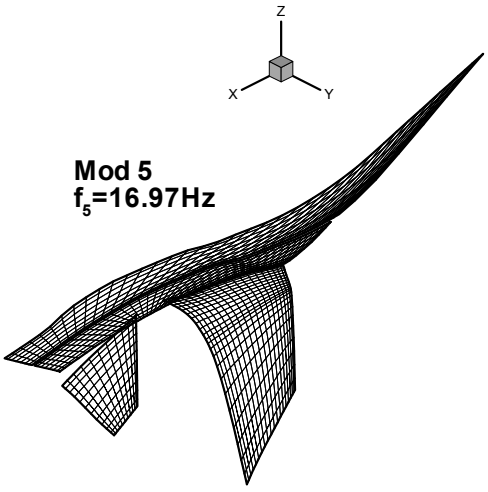

(4e)

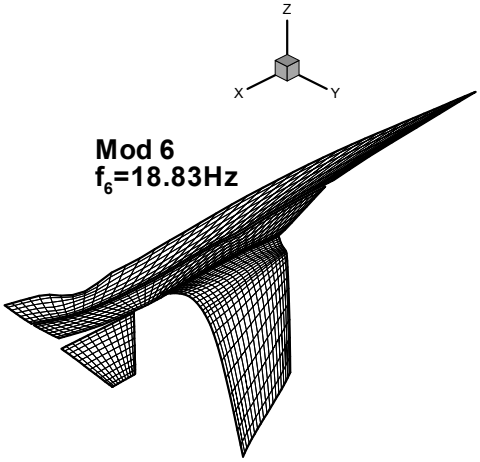

(4f)

Fig. 4 First six modes and natural frequencies

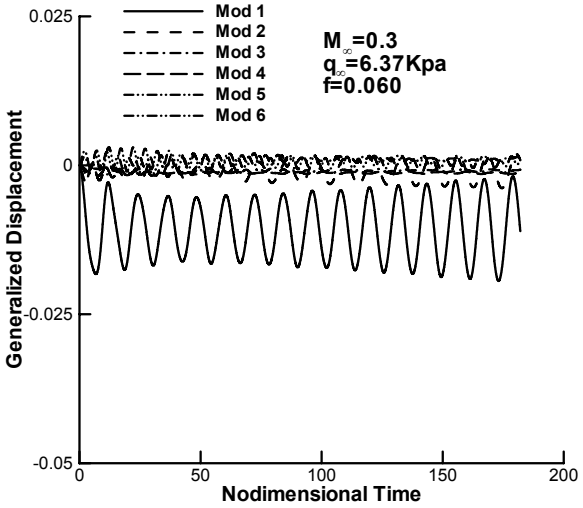

(5a)

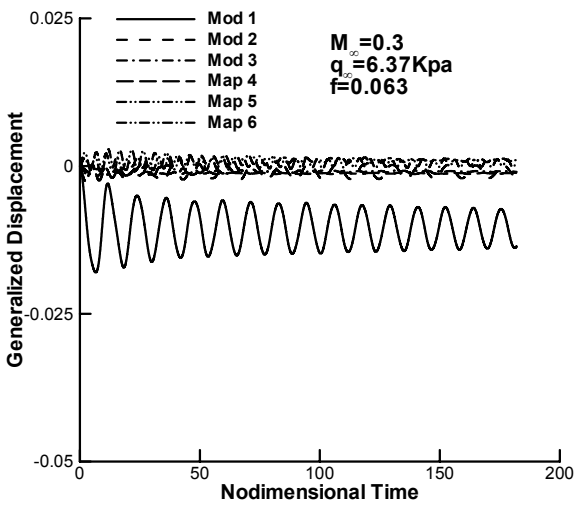

(5b)

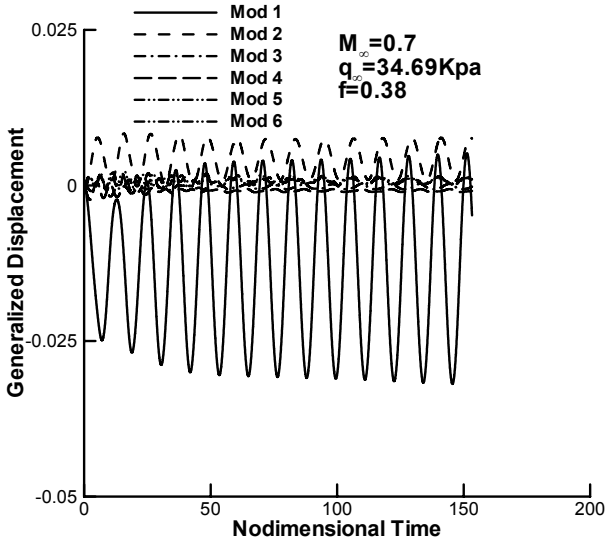

(5c)

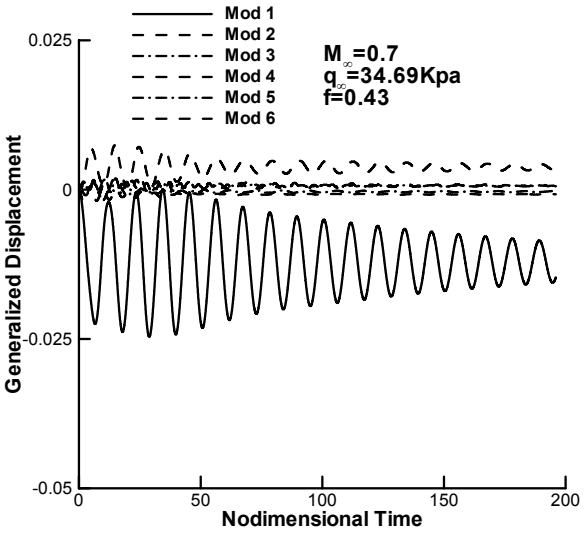

(5d)

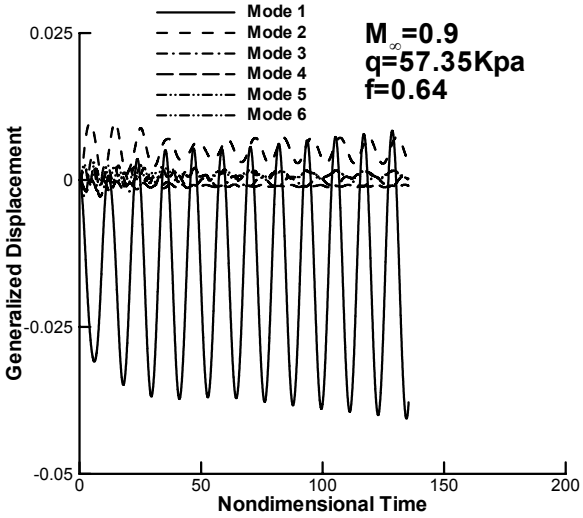

(5e)

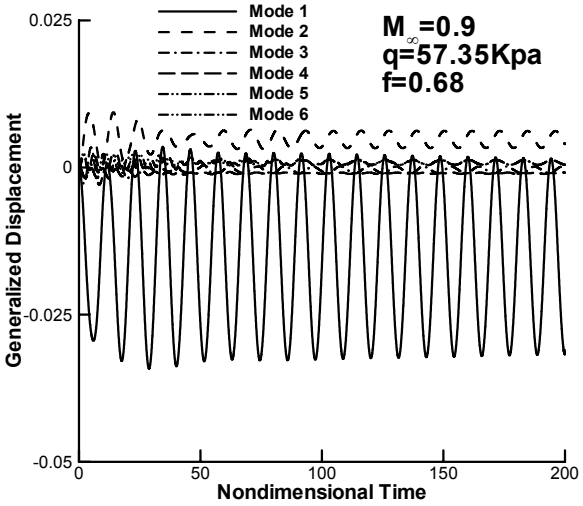

(5f)

Fig. 5 Dynamic response of first six modes at Mach number s of 0.3, 0.7, 0.9

2. A Complex Aircraft Model The second calculation is taken for the configuration of Fig. 1. The first six structural modes and their natural frequencies are shown in Fig. 4. Due to the full movement of horizontal wing, the calculation is easy to diverge for some cases, therefore a special treatment has been done for the grid deformation in the blocks between the fuselage and the horizontal wing.

For the case, flutter is analyzed with the change of structural stiffness, namely, the freestream density and freestream temperature are assumed unchangeable(such as at the sea level), then dynamic pressure can be calculated for different Mach number. Under the fixed Mach number and dynamic pressure, a stiffness coefficient of f_i can be introduced into the structural equation of motion as

$$\ddot{q}_i + 2\zeta_i \omega_i \dot{q}_i + f_i \omega_i^2 q_i = [\Phi]_i^T F / M_i \tag{11}$$

such as when $f_i = 0.7$, it is indicated that the structural stiffness calculated is only 70 percent of the original stiffness. For different stiffness coefficient, the dynamic responses may be convergence or divergence, then we can estimate the value of stiffness coefficient at the flutter boundary.

The dynamic responses of different stiffness and freestream Mach numbers are shown in Fig. 5. The dominant mode appears to be the first bending mode, and only the second mode has some effects to the first mode. The response of the first mode is analyzed. At Mach number of 0.3, the dynamic response deverges at $f_i = 0.060$ and converges at $f_i = 0.063$, then the stiffness coefficient of flutter boundary should be at $0.060 < f_i < 0.063$ and the nondimensional frequency at $0.08626 < k < 0.08905$. Similarly, at Mach number of 0.7, the dynamic response deverges at $f_i = 0.38$ and converges at $f_i = 0.43$, then the stiffness coefficient of flutter boundary should be at $0.38 < f_i < 0.43$ and the nondimensional frequency at $0.08905 < k < 0.09183$. At Mach number of 0.9, the dynamic response deverges at $f_i = 0.64$ and converges at $f_i = 0.68$, then the stiffness coefficient of the flutter boundary should be at $0.64 < f_i < 0.68$ and the nondimensional frequency at $0.08626 < k < 0.08905$. Through the comparision, it is indicated that flutter may be occur with the structural design of 70 percent original stiffness at Mach number of 0.9, which is also the limitation of structural design to avoid flutter.

CONCLUDING REMARKS

A fully implicit aeroelastic solver has been developed for fluid/structure interaction of flutter on complex configuration through the tightly coupled solution of Navier-Stokes equations and structural equations of motion. Navier-Stokes equations are discretized with a LU-SGS subiteration algorithm and the modified HLLEW scheme. Structural equations of motion are discretized directly by a second scheme with subiteration in generalized coordinates. Multiblock grid deformation is performed with the TFI method. IPS and the principle of virtual work are used for data transformation of deformation and force between the fluids and the structures. Two aerodynamic models including the AGARD 445.6 standard aeroelastic wing, a complex aircraft configuration have been simulated with the present solver. It is indicated the calculated results are acceptable and the developed code can treat the problems of complex fluid/structure interaction.

REFERENCES

[1] G. P. Guruswamy, *Vortical flow computations on swept flexible wings using Navier-Stokes equations,* AIAA Journal, Vo. 28, (1990), pp.2077-2084.

[2] E. M. Lee-Rausch, J. T. Batina, *Wing flutter computations using an aeroelastic model based on the Navier-Stokes,* Journal of Aircraft, Vol.33, (1996), pp.1139-1147.

[3] P. M. Hartwich, S. K. Dobbs, A. E. Arslan, S. C. Kan, *Navier-Stokes computations of limit-cycle oscillations for a B-1-Like configuration*, Journal of Aircraft, Vol. 38, No.2, (2001), pp.239-247.

[4] S. A. Goodwin, R. A. Weed, L. N. Sankar, P. Raj, *Towards cost-effective aeroelastic analysis on advanced parallel computing systems,* Journal of Aircraft, Vol. 36, No. 4, (1999), pp. 710-715

[5] J. J. Alonso, A. Jameson, *Fully-implicit time-marching aeroelastic solutions*, AIAA Paper 94-0056. (1994).

[6] F. Liu, J. Cai, Y. Zhu, H. M. Tsai, A. S. F. Wong: *Calculation of wing flutter by a coupled fid-tructure mthod,* Journal of Aircraft, Vol. 38, No.2, (2001) pp.334-242.

[7] G. S. L. Goura, K. J. Badcock, M. A. Woodgate, B. E. Richards, *Implicit mthod for the tme marching analysis of flutter*, The Aeronautical Journal, Vol. 105, (2001), pp.199-214.

[8] R. B. Melville, S. A. Morton, D. P. Rizzetta, *Implementation of a fully-implicit, aeroelastic Navier-Stokes solver,* AIAA paper 97-2039, (1997).

[9] R. E. Gordiner, R. B. Melville, *Transonic flutter simulations using an implicit aeroelastic solver,* Journal. of Aircraft, Vol.37, (2000), pp.872-879.

[10] M. A. Potsdam, G. P. Guruswamy, *A parallel multiblock mesh movement scheme for complex aeroelastic applications,* AIAA Paper 01-0716. (2001).

[11] A. S. F. Wong, H. M. Tsai, J. Cai, Y. Zhu, F. Liu, *Unsteady flow calculations with a multi-block moving mesh algorithm,* AIAA Paper 00-1002. (2000).

[12] R. L. Harder, R. N. Desmarais, *Interpolation using surface splines,* Journal of Aircraft, Vol. 9, (1972), pp.189-191.

[13] K. Appa, *Finite-surface spline*, Journal of Aircraft, Vol. 26, (1989), pp.495-496.

[14] G. S. L. Goura, K. J. Badcock, M. A. Woodgate, B. E. Richards, *A data exchange method for fluid-structure interaction problems,* The Aeronautical Journal, Vol. 105, (2001), pp.215-221.

[15] G. W. Yang, S. Obayashi, *Transonic aeroelastic calculation with full implicit subiteration and deforming grid approach, aeronautical numerical simulation technology symposium*, (2001), Tokyo, June, 2001.

[16] Guowei Yang, Shigeru Obayashi, Jiro Nakamichi, *Aileron buzz simulation using an implicit multibolk aeroelastic solver,* Journal of Aircraft, Vol. 40, No. 3, p.580-589, (2003).

[17] P. D. Thomas, C. K. Lombard, *Geometric conservation law and its application to flow computations on moving grids*, AIAA Journal, Vol. 17, No. 10, (1979), pp.1030-1037.

[18] S. Yoon, A. Jameson, *Lower-upper symmetric –Gauss-Seidel ,ethod for the Euler and Navier-Stokes equations,* AIAA Journal Vol. 26, (1988), pp. 1025-1026.

[19] S. Obayashi, G. P. Guruswamy, *Convergence acceleration of a Navier-Stokes solver for efficient static aeroelastic computations,* AIAA Journal, Vol.33, (1995), pp.1134-1141.

[20] D. P. Rizzetta, M. R. Visbal, *Comparative numerical study of two turbulence ,odels for airfoil static and dnamic sall.* AIAA Journal, Vol.31, (1993), pp.879-889.

[21] R. Zwaan, *LANN Wing Pitching Oscillation*, AGARD-R-702, (1988).